Drug Design, Development and Therapy

Dovepress
Taylor & Francis Group

Open Access Full Text Article

ORIGINAL RESEARCH

Regulatory Effects of Zhenxin Formula in Treating Doxorubicin-Induced Heart Failure: Network Pharmacology and Animal Experimental Verification

Qiong Wu[1,*], Hao Wang[2,*], You Hua Wang[1], Jun Du[3], Bo Li[3], Xiao-Na Gan[3], Chen-Yang Liu[2], Jing Liang[2], Chang Liu[2], Min Cao[2]

[1]Department of Cardiology, Longhua Hospital Affiliated to Shanghai University of Traditional Chinese Medicine, Shanghai, People's Republic of China; [2]Department of Emergency, Longhua Hospital Affiliated to Shanghai University of Traditional Chinese Medicine, Shanghai, People's Republic of China; [3]Nutrilite Health Institute, Amway (China) R&D Center, Shanghai, People's Republic of China

*These authors contributed equally to this work

Correspondence: Chang Liu; Min Cao, Department of Emergency, Longhua Hospital Affiliated to Shanghai University of Traditional Chinese Medicine, Xunhui, 725 South Wan-Ping Road, Shanghai, 200032, People's Republic of China, Tel +862164385700, Email doctorlchang@163.com; caomin_cm@163.com

Objective: This study aimed to elucidate the mechanisms underlying the protective effects of Zhenxin Formula (ZXF) against doxorubicin (Dox)-induced HF through the integration of network pharmacology, phospho-antibody array analysis, and experimental validation.

Methods: The active components and potential targets of ZXF were identified via the Traditional Chinese Medicine Systems Pharmacology (TCMSP) platform, while HF-associated target genes were retrieved from the OMIM, Genecards, and TTD databases. Protein-protein interaction (PPI) networks and compound-disease target networks were constructed using Cytoscape 3.7.2, with functional annotations performed through GO enrichment and KEGG pathway analyses using R software. Experimental validation involved the establishment of a Dox-induced HF model via intraperitoneal injection, with ZXF's therapeutic effects evaluated using cardiac ultrasound, morphological staining, and Western blot analysis. Additionally, a phospho-antibody array was utilized to screen over 300 molecules across 16 canonical signaling pathways in ZXF-treated HF models, with Western blot analysis confirming the specific pathways implicated in ZXF's therapeutic effects.

Results: Network pharmacology analysis identified 56 potential active ingredients in ZXF, 47 of which were associated with HF-related targets. AKT1 emerged as the target most strongly correlated with HF improvement. In vivo, ZXF significantly enhanced cardiac function and mitigated myocardial fibrosis and cardiomyocyte apoptosis. Phospho-antibody array analysis revealed that 16 phosphorylated proteins were upregulated and 3 downregulated in the Dox-treated group. ZXF intervention resulted in the upregulation of 10 phosphorylated proteins and downregulation of 5. Comparative analysis highlighted PDK1-Phospho and FOXO1/3/4-Phospho as pivotal phosphorylated proteins mediating ZXF's cardioprotective effects. Western blot analysis confirmed that ZXF enhanced phosphorylation levels of PI3K, PDK1, AKT, and FOXO1 in the Dox-induced HF model.

Conclusion: This study, employing network pharmacology, phospho-antibody array analysis, and experimental validation, demonstrates that ZXF ameliorates cardiac dysfunction and suppresses myocardial apoptosis in Dox-induced HF through modulation of the PI3K/PDK1/AKT/FOXO1 signaling pathway.

Keywords: network pharmacology, phospho-antibody array, Zhenxin Formula, heart failure, PI3K/PDK1/AKT/FOXO1 signaling pathway

Introduction

Heart failure (HF) is a complex clinical syndrome characterized by impaired ventricular filling and/or ejection function (EF) resulting from diverse causes.[1,2] It represents not only the terminal stage of heart disease but also a frequent comorbidity and endpoint in the progression of various non-cardiogenic conditions. With its high prevalence, significant

Received: 3 February 2025
Accepted: 25 June 2025
Published: 12 July 2025

risk of sudden death, and poor prognosis, HF poses a substantial global public health challenge.[3,4] A pivotal contributor to HF development is myocardial remodeling, a process marked by cardiomyocyte hypertrophy and fibrosis. This process is driven by a complex interplay of mechanisms, including apoptosis, inflammation, autophagy, ferroptosis, and other detrimental factors.

Zhenxin Formula (ZXF) is a traditional Chinese medicine (TCM) formula used by Longhua Hospital affiliated to Shanghai University of TCM for the prevention and treatment of chronic HF. TCM has a long history of being utilized in HF treatment.[5–7] According to TCM principles, HF originates from congenital deficiency or post-illness disorders, culminating in heart yang deficiency, which is a central pathological factor in its progression. ZXF, a classic TCM formula, comprises ingredients such as Shan Zhu Yu (*Cornus officinalis Sieb. et Zucc.)*, Gui Zhi (*Cinnamomum cassia Presl.)*, Fu Zi (*Aconitum carmichaelii Debx.)*, Bai Shao (*Paeonia lactiflora Pall.)*, and Ze Lan (*Eupatorium japonicum Thunb.)*. Renowned for warming and invigorating heart yang, transforming qi, and promoting diuresis, ZXF has shown clinical efficacy in HF treatment.[8] However, its precise molecular mechanisms remain unclear.

Advancements in bioinformatics and systems biology have highlighted network pharmacology as a pivotal tool for identifying active ingredients and unraveling therapeutic mechanisms, particularly for the "multi-compound, multi-target" nature of TCM. By constructing disease-gene-target-drug networks, this approach offers comprehensive insights.[9,10] However, limitations in TCM databases, such as incomplete active compound data and insufficient molecular target coverage, hinder detailed analyses.[11] Phospho-antibody arrays address these gaps by detecting and quantifying phosphorylated proteins, crucial post-translational modifications in cell signaling. This high-throughput technology validates computational predictions by mapping dynamic signaling changes in disease models.[12,13] The integration of network pharmacology and phospho-antibody arrays enhances bioinformatics' predictive power with experimental validation, providing a robust framework to explore therapeutic mechanisms and advance TCM-based treatment strategies.

In this study, we explored the active components and mechanisms underlying the therapeutic effects of ZXF on HF. Through a combined network pharmacology and phospho-antibody array approach, we elucidated the material basis and signaling pathways involved in ZXF's action. Subsequent experiments employing Dox-induced HF models were conducted to validate these findings, offering deeper insights into the potential mechanisms by which ZXF mitigates HF progression.

Materials and Methods

Investigation of the Mechanism of ZXF Against HF via Network Pharmacology

Screening the Active Ingredients and Target Prediction of ZXF

The potential active ingredients within TCM compound prescriptions were retrieved from the TCMSP database (TCMSP, http://lsp.nwsuaf.edu.cn/tcmsp.php). Using oral bioavailability (OB ≥ 30%) and drug likeness (DL ≥ 0.18) as screening criteria. The corresponding targets of these components were also sourced from the TCMSP database, and their names were standardized and harmonized using the UniProt database (https://www.uniprot.org/uniprot/) to ensure consistency. Furthermore, the molecular structures of the mentioned components were acquired from the TCMSP database and subsequently imported into the Swiss Target Prediction database (http://www.swisstargetprediction.ch/). From this prediction, targets with scores exceeding 0 were selectively identified as potential drug targets.

Analysis of Gene Expression Differences Between Healthy Individuals and Patients with Heart Failure

Utilizing the OMIM (https://omim.org/), Genecards (https://www.genecards.org/), and TTD (https://db.idrblab.net/ttd/) databases, we conducted a keyword search for "Heart Failure" to identify relevant disease targets. Subsequently, both the drug targets and disease targets were uploaded into the Venny 2.1 online software visualization tool platform, where a Venn diagram was generated to illustrate the overlapping and unique targets. This study uses publicly available datasets, which are exempt from ethical review in accordance with Article 32, Items 1 and 2 of the Measures for Ethical Review of Life Science and Medical Research Involving Human Subjects (issued on February 18, 2023, China).

Reconstruction of Compound-Target Network and Protein-Protein Interaction Network

Using Cytoscape 3.9.1 software, a comprehensive " TCM - Ingredient - Target" network graph to construct network graph. The Network Analyzer functionality was leveraged to meticulously analyze the key active ingredients within the TCM compound recipe. Subsequently, the identified common targets were introduced into the STRING database (https://string-db.org) for retrieval, with specific parameters set to "Homo sapiens" for protein species and a minimum interaction threshold of 0.9. The retrieved target interaction network data was then integrated into Cytoscape software to generate a PPI network graph. In this graph, the size and color intensity of each node were dynamically adjusted based on their degree values, providing a visual representation of their relative importance. To further refine our analysis, the PPI network was imported into Cytoscape 3.9.1, where topological analysis was conducted using the Network Analyzer tool. Core targets were identified based on their degree values, with higher values indicating a more pivotal role in the network.

GO Enrichment Analysis and KEGG Pathway Analysis

We conducted GO enrichment analysis and KEGG pathway analysis on the shared targets utilizing the David database (https://david.ncifcrf.gov). The enrichment outcomes were subsequently visualized into bar charts and bubble plots using R language for clarity and comprehension. Following the KEGG enrichment analysis of the common targets with the David database, a compilation of KEGG pathways was derived. Select the top 20 pathways with P-values within 0.05 to create bar charts and bubble plots for KEGG enrichment. The -log10 (P-value) represents the significance of the enrichment, with redder colors indicating higher significance.

High-Performance Liquid Chromatography (HPLC)

ZXF comprises 12 g of Shan Zhu Yu (Cornus officinalis Sieb. et Zucc.), 10 g of Gui Zhi (Cinnamomum cassia Presl.), 12 g of Fu Zi (Aconitum carmichaelii Debx.), 15 g of Bai Shao (Paeonia lactiflora Pall.), and 12 g of Ze Lan (Eupatorium japonicum Thunb.), all sourced from Sichuan Xinlvse Pharmaceutical Technology Development Co., Ltd. The formula was prepared by double reflux extraction using water (10:1, volume/weight) for 2 hours per cycle. The combined filtrates were concentrated to 1.5 g/mL. For HPLC, five ZXF samples (25 mg/mL) were prepared with varying methanol-water ratios: water, 30%, 50%, 70%, and 100% methanol. Each sample underwent 30 minutes of ultrasonic treatment, followed by centrifugation at 16,000 rpm for 5 minutes. Supernatants were stored in chromatographic vials. HPLC analysis employed an HSS T3 column with a mobile phase of 0.1% acetic acid in water and acetonitrile. Detection wavelengths were 254 nm and 330 nm, with a flow rate of 0.3 mL/min and injection volume of 1μL.

Regents

Doxorubicin (HY-15142) was purchased from MedChemExpress. Captopril (No. H31022986) was purchased from Shanghai Bristol-Myers Squibb Pharmaceuticals Co., Ltd). Anti-Fas antibody (ab82419) was purchased from Abcam. Anti-Bax antibody (ARG66247) and anti-Bcl-2 antibody (ARG55188) were purchased from Arigo. Anti-Caspase-3 antibody (D3R6Y), anti-AKT1 phospho (Thr308) antibody (4056S), anti-AKT1 antibody (2920S), anti-FOXO1 phospho (Ser256) antibody (9461T), anti-FOXO1 antibody (2880T), anti-PDK1 phospho (Ser241) antibody (3438T), and anti-PDK1 antibody (5662S) were purchased from CST. Anti-PI3K phosphor (Tyr607) antibody (Abs130868) was purchased from Absin. Anti-PI3K antibodies (S0B0265) was purchased from Starter. Anti-GAPDH antibody (G9545) was purchased from Sigma.

Animals Experiment

Forty-six male Wistar rats, weighing between 170–220 grams, were procured from the Experimental Animal Center of Shanghai University of TCM, Certificated number SYXK (Hu) 2014-0008. These animals were raised under controlled conditions of a 12-hour light/dark cycle, with an ambient temperature of 21±2 °C and a relative humidity ranging from 30% to 70%. They had ad libitum access to standard rodent feed and water. Animal experiments were approved by the Animal Care Committee of the Shanghai University of TCM (Approval Number: PZSHUTCM210312009), and all procedures adhered strictly to the guidelines set forth by the Institutional Animal Care and Use Committee (IACUC).

Based on our previous work and established protocols, a widely recognized doxorubicin-induced heart failure model was employed.[14–16] After a 7-day acclimatization period, 46 rats were randomly assigned using a random number table into two groups: 10 rats in the negative control (Con) group and 36 rats in the experimental group. The experimental group received weekly intraperitoneal injections of doxorubicin solution (1 mg/mL) at a dose of 2.5 mg/kg for six consecutive weeks, while the control group received equivalent volumes of 0.9% saline. After six weeks, heart failure in the experimental group was confirmed by echocardiography, as evidenced by significant reductions in EF, fractional shortening (FS), stroke volume (SV), and cardiac output (CO), along with increased left ventricular end-systolic diameter (LVESD) and end-diastolic diameter (LVEDD).[17–19] The 36 model-confirmed rats were subsequently randomized into three groups (n = 12 per group): the model group (Dox), the ZXF treatment group (ZXF), and the captopril treatment group (Cap). ZXF was administered at a dose of 3.6 g/(kg·d), based on previous clinical studies.[8] Captopril was administered at a dose of 5 mg/(kg·d). The Con and Dox groups received equivalent volumes of distilled water daily. All treatments lasted for four consecutive weeks. Throughout the experiment, the rats were closely monitored on a daily basis for general health indicators, including mental status, food intake, physical activity, urine and fecal output, coat condition, and mortality.

Echocardiography

After 4 weeks of intervention, rats were anesthetized with 3% pentobarbital sodium (1.17 mL/kg, intraperitoneally) and positioned supine. An ultrasound probe was placed on the left chest, and M-mode images were obtained using two-dimensional ultrasound guidance. Cardiac parameters, including EF, FS, LVEDD, LVESD, SV, and CO, were measured over three consecutive cardiac cycles.

Histological Analysis

After 4 weeks of treatment, the rats were euthanized via intraperitoneal injection of 3% sodium pentobarbital (150 mg/kg). Within 2 minutes post-injection, respiratory arrest occurred, followed by cardiac arrest and pupillary dilation, confirming death. The hearts were then excised, with arteries and major blood vessels removed, and the left ventricular myocardial tissue was isolated. Portions of the tissue were soaked in formalin for pathological examination, while the remaining tissue was stored at −80°C. Formalin-fixed myocardial tissues were paraffin-embedded, sectioned into 5 μm slices, and stained with hematoxylin and eosin (HE) for histopathological analysis. To evaluate collagen deposition, sections were dewaxed and stained with Masson's trichrome. Images were captured using a microscope (CFM, Olympus) at 400× magnification, with five fields per section analyzed. Collagen volume fraction (CVF) was quantified using Image Pro Plus 6.0 software, calculated as the mean ratio of connective tissue area to total tissue area, excluding perivascular fibrotic tissues.

Immunohistochemistry

After dewaxing paraffin sections and rehydrating them, antigen retrieval and blocking were performed. Subsequently, 50μL of primary antibody (Fas, 1:1000) was applied at 37°C for 60 minutes, followed by incubation with a biotinylated secondary antibody at 37°C for 30 minutes. After color development, counterstaining, dehydration, and clearing, the slides were sealed. Images were captured and analyzed using OlyVIA software, with five different fields of view selected per section. The percentage of positive staining relative to the total area was calculated using Image Pro Plus 6.0 software.

Phospho-Antibody Array

Phosphoprotein profiling by the signaling phospho-antibody microarray—CSP100plus, which was designed and manufactured by Full Moon Biosystems, Inc. (Sunnyvale, CA), contains 304 antibodies. Each of the antibodies has six replicates that are printed on coated glass microscope slides, along with multiple positive and negative controls. The antibody array experiment was performed by Wayen Biotechnology (Shanghai, China), according to their established protocol. The fluorescence signal of each antibody was obtained from the fluorescence intensity of antibody-stained regions. A ratio computation was used to measure the extent of protein phosphorylation. The phosphorylation ratio was

calculated as follows: phosphorylation ratio= phospho value/non-phospho value. The total proteome ratios were standardized by Tubulin-b.

Western Blotting

Take an appropriate amount of rat myocardial tissue stored at −80°C, and after pretreatment, homogenize and lyse the tissue. Centrifuge the lysate and determine the total protein concentration. Prepare a 10% separating gel and 5% stacking gel for electrophoresis. Following electrophoresis, transfer the proteins to a membrane and block with 5% BSA at room temperature for 2 hours. Incubate the membrane overnight with primary antibodies, including PDK1 (1:1000), p-PDK1 (1:1000), PI3K (1:1000), p-PI3K (1:1000), AKT (1:1000), p-AKT (1:1000), FoxO1 (1:1000), p-FoxO1 (1:700), Caspase3 (1:1000), Bcl-2 (1:1000), Bax (1:1500), FAS (1:1000), and GAPDH (1:2000). After washing, incubate with a secondary antibody (1:2000) at room temperature, wash again, and visualize the target proteins.

Statistical Analysis

Quantitative data conforming to a normal distribution were presented as mean± SD ($\bar{\chi} \pm s$). When the measurement data satisfies the test of homogeneity and normality of variance, a one-way analysis of variance (ANOVA) was subjected for comparison between more than two groups, and the LSD-*t* test was used for comparisons between groups. If the measurement data could not satisfy the test of homogeneity or normality of variance, a nonparametric rank-sum test was used. All analyses were performed using GraphPad Prism version 8.0. A value of $P<0.05$ was considered to be significant.

Results

Network Pharmacology-Based Strategy for Predicting Potential Targets of ZXF for Treating HF

Active Compounds in ZXF and Their Targets

In the TCMSP and TCMID databases, 56 active compounds with OB (oral bioavailability) ≥ 30% and DL (drug-likeness) ≥ 0.18 were identified (Supplementary Table S1). A total of 752 targets of these active compounds were retrieved from the TCMSP database (Supplementary Box 1). Disease targets were collected from OMIM (664), Genecards (620), and TTD (38) databases. After deduplication, 1206 unique disease targets were obtained (Supplementary Box 2). Using the Venny 2.1 online platform, we generated a Venn diagram by intersecting the 752 drug targets with 1206 disease targets, resulting in 120 common drug-disease targets (Figure 1). Subsequently, we constructed a "Traditional Chinese Medicine-Compounds-Targets" network in Cytoscape by linking the 56 potential active components with the 120 common targets. After removing 9 isolated components without target connections, we retained 47 potential active components for the final network visualization (Figure 2).

Candidate Targets and PPI Network Analysis

The aforementioned 120 common targets were then imported into the STRING database for retrieval. By setting the protein species to "Homo sapiens" and the minimum interaction score threshold to 0.9, we obtained network relationship data for the interactions between these targets. This data was then imported into Cytoscape software to create a protein-protein interaction (PPI) network diagram. In this diagram, the size and color intensity of the nodes varied according to their degree values, with the outermost circle representing targets with a degree greater than or equal to 10. The diagram contained 95 nodes and 185 edges (Figure 3A). The PPI network was imported into Cytoscape 3.9.1, and a topological analysis was performed using the network analyzer tool. A bar chart was generated using R 4.2.1 to represent the top 20 targets with the highest Degree values (Figure 3B). The PPI network analysis revealed that AKT1 may be the most important potential target for ZXF in the treatment of HF (Degree = 16).

GO Enrichment Analysis and KEGG Signaling Pathway Analysis

After performing GO enrichment analysis on the 120 common targets using the David database, we obtained three main categories: biological processes, cellular components, and molecular functions. The GO results showed that the

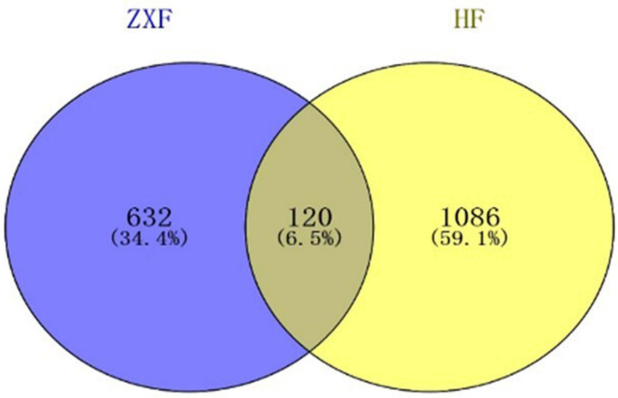

Figure 1 Screening of Drug-Disease Common Targets. In the figure, the purple circles represent drug targets of ZXF, the yellow circles denote heart failure (HF)-related disease targets, and their intersecting area indicates the shared drug-disease common targets.

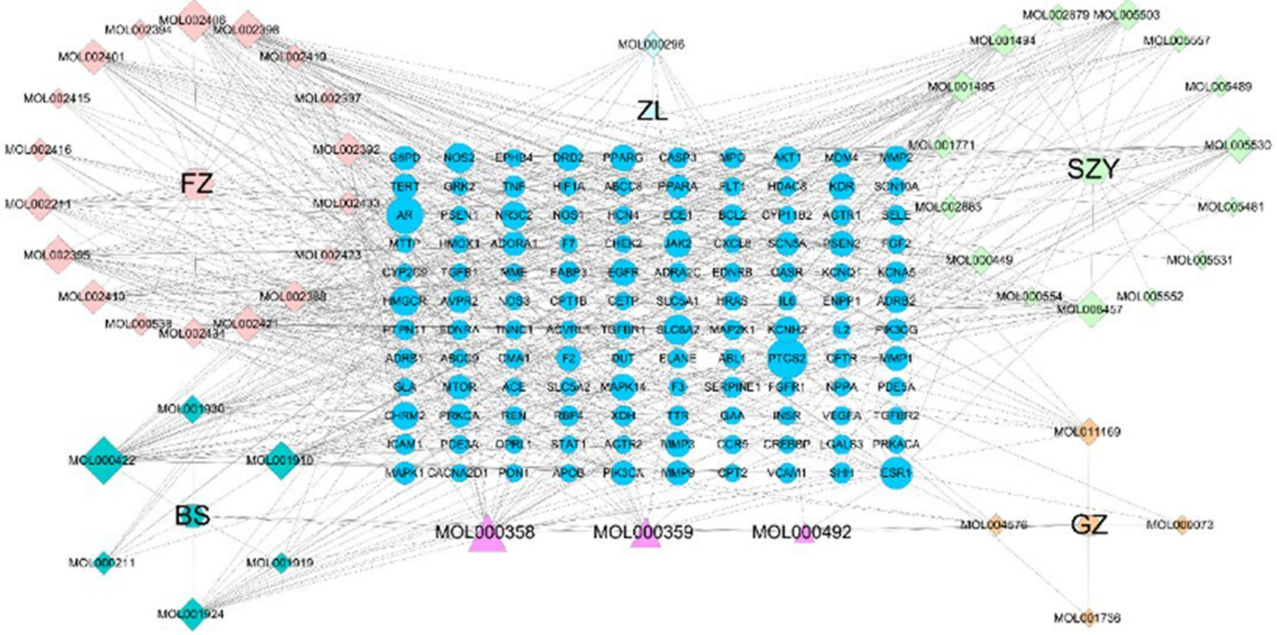

Figure 2 Screening of Drug-Disease Common Targets. Hexagonal nodes represent herbal medicines; diamond nodes represent unique components of each herb; triangular nodes represent shared components (9 active components without target-disease intersections were removed, while 47 effective components are highlighted in red in Supplementary Table S1); circular nodes represent the 120 common targets. Node sizes vary according to their degree values.

intersecting genes were enriched in 662 biological process pathways, 67 cellular component expression processes, and 113 molecular function-related processes. We selected the top 10 pathways with the lowest P-values in each category to create bar charts and bubble plots (Figure 4).

Based on the GO enrichment analysis of the intersecting genes, the results suggest that ZXF is involved in several biological processes, including response to hypoxia, regulation of the MAPK cascade and the gene expression. Additionally, ZXF's impact on cellular components is primarily associated with the plasma membrane, cell surface, and membrane rafts. Moreover, it is closely associated with endopeptidase activity, protein homodimerization, and transcription coactivator binding (Figure 4A). After conducting KEGG enrichment analysis on the 120 common targets using the David database, we obtained a total of 159 KEGG pathways, including AGE-RAGE signaling pathway in diabetic complications, Pathways in cancer, HIF-1 signaling pathway, etc. We selected the top 20 pathways with the lowest P-values to create bar charts and bubble plots for KEGG enrichment (Figure 4B).

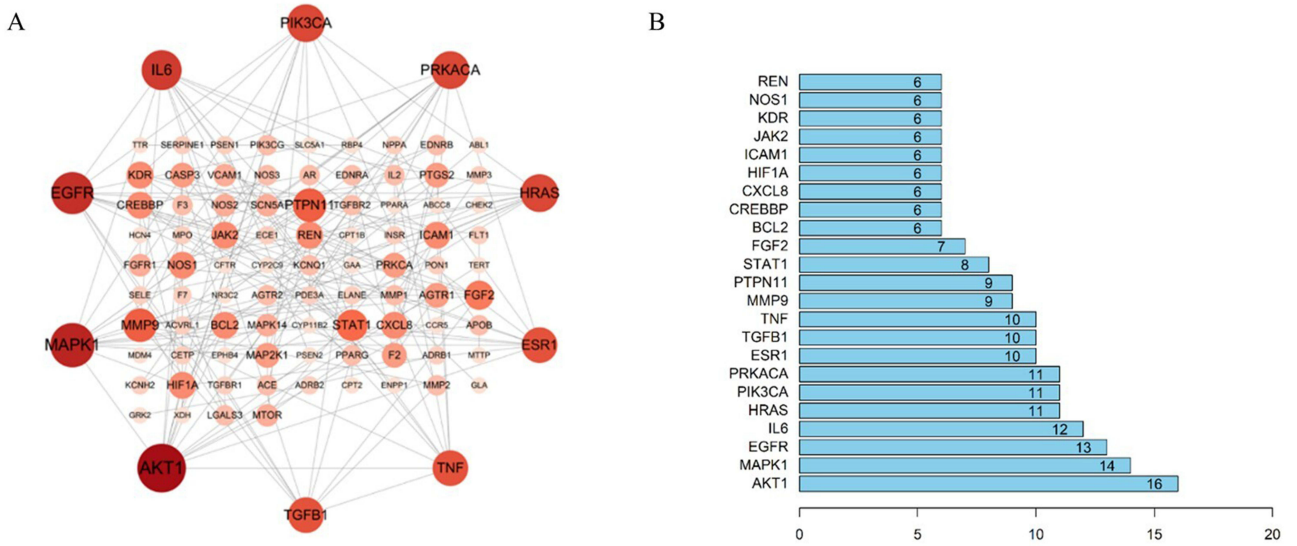

Figure 3 Network Pharmacology Analysis Identifies Hub Targets of ZXF. (**A**) Node size and color intensity vary according to their Degree values, with the outermost circle representing targets having Degree ≥ 10. (**B**) Ranking of Core Targets Based on PPI Topological Analysis (Top 20 by Degree). The bar graph illustrates the Degree values of the targets.

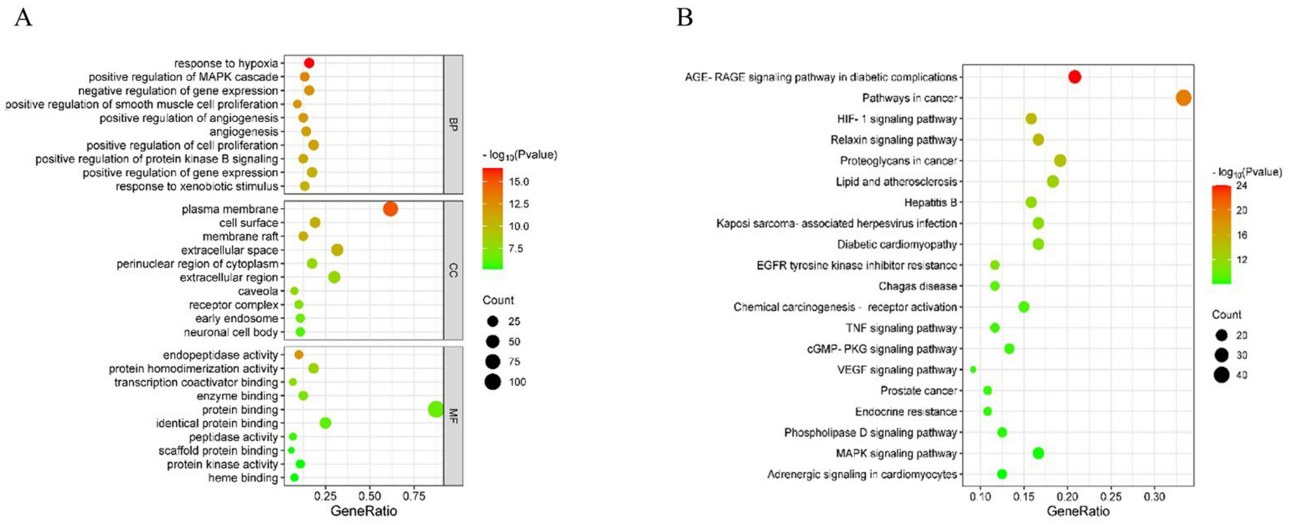

Figure 4 Enrichment Analysis of Identified Targets and KEGG Pathway Analysis for ZXF. Enrichment Analysis of Identified Targets and KEGG Pathway Analysis for ZXF. (**A**) GO enrichment analysis of ZXF for heart failure treatment. The y-axis represents three categories: biological processes, cellular components, and molecular functions; the x-axis shows gene percentage; circle size corresponds to gene count, while color indicates significance. (**B**) KEGG enrichment analysis of ZXF compound for heart failure treatment. The y-axis displays pathways, the x-axis shows gene percentage, with circle size representing gene count and color indicating significance.

Quality Control of ZXF Using High-Performance Liquid Chromatography

ZXF is a traditional Chinese medicine compound containing a variety of chemical ingredients. To control its quality, we first constructed a component-target-pathway network diagram using Cytoscape to predict its effective components. The results indicated that kaempferol, paeoniflorin, and catechin may be the main active components, with active contents of 33, 17, and 4, respectively (Supplementary Table S2). We then conducted HPLC analysis to determine the contents of these components. As shown in Figure 5, The content of catechin in the ZXF extract was 0.09%, with a retention time of 11.304 minutes and peak area of 13870 μV*sec. The content of paeoniflorin in the ZXF extract was 1.18%, with a retention time of 14.221 minutes and peak area of 111901 μV*sec. Additionally, kaempferol was not detected in the ZXF extract.

https://doi.org/10.2147/DDDT.S513643

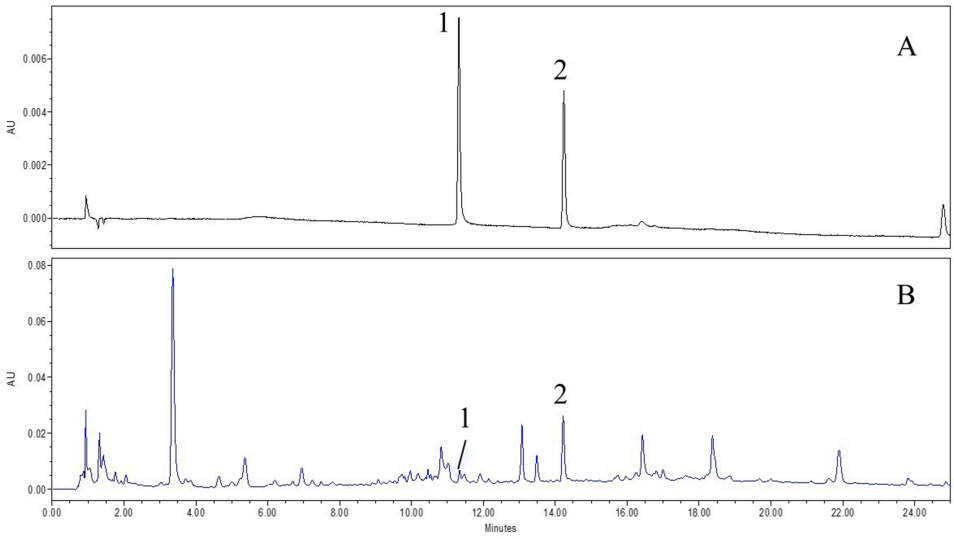

Figure 5 Chromatogram of catechin and paeoniflorin standards versus ZXF extract. Chromatogram of catechin and paeoniflorin standards versus ZXF extract. ((**A**) reference standard solution, (**B**) sample solution; 1 - catechin, 2 – paeoniflorin).

ZXF Improves Cardiac Function

We evaluated the effects of ZXF on cardiac function in a Dox-induced HF model (Figure 6A). Echocardiographic assessments were conducted on all rats at the end of the 10-week study period (Figure 6B–G). Compared with the control group, the Dox group showed significant reductions in EF, FS, CO, and SV, along with marked increases in LVESD and LVEDD, indicating impaired cardiac function caused by Dox intraperitoneal injection. In contrast, ZXF treatment significantly improved cardiac function, evidenced by notable enhancements in EF, FS, CO, and SV, as well as significant reductions in LVESD and LVEDD, comparable to the effects observed in the Cap group.

ZXF Attenuates Myocardial Inflammation and Fibrosis

The protective effects of ZXF were assessed using HE staining and Masson trichrome staining of heart sections (Figure 7A). HE staining revealed severe inflammatory cell infiltration and myocardial structural disorganization in the Dox group, while ZXF treatment significantly reduced inflammatory cell infiltration, indicating its anti-inflammatory effects (Figure 7A). Masson trichrome staining showed extensive collagen deposition in the Dox group, with prominent fibrotic tissue in the myocardial interstitium. Quantification of CVF revealed a significant increase in the Dox group compared to the control group. However, ZXF treatment markedly reduced CVF levels compared to the Dox group, demonstrating an even greater effect than Captopril. (Figure 7B). These results suggest that ZXF protects against Dox-induced HF by mitigating myocardial inflammation and fibrosis.

ZXF Inhibited Cardiomyocyte Apoptosis

Immunohistochemical staining was conducted to evaluate the effect of ZXF on cardiomyocyte apoptosis (Figure 7A). Fas expression, which was significantly elevated in the Dox group, was markedly decreased following ZXF treatment (Figure 7C). Western blot analysis further confirmed these findings in the Dox-induced HF model. As shown in Figure 8A–E, the levels of pro-apoptotic proteins Bax, Caspase-3, Fas were significantly higher in the Dox group compared to the control group, but ZXF intervention significantly reduced their expression. Conversely, the anti-apoptotic protein Bcl-2, which was notably downregulated in the Dox group, was significantly upregulated with ZXF treatment. These results demonstrate that ZXF exerts a protective anti-apoptotic effect on cardiomyocytes.

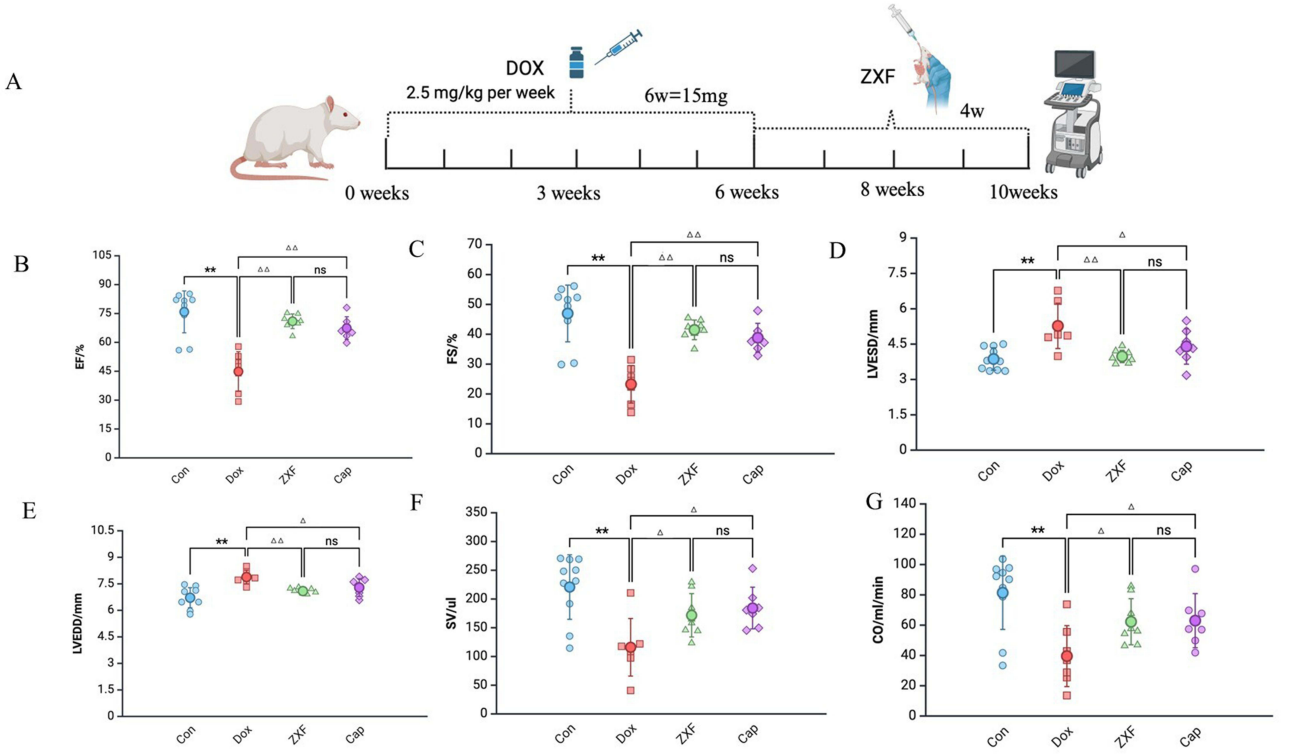

Figure 6 ZXF Improves Cardiac Function. (**A**) Animal experimental strategy. (**B**–**G**) Statistical results of EF, FS, LVESD, LVEDD, CO, SV. **P<0.01 vs Con group; $^{\Delta}P$<0.05, $^{\Delta\Delta}P$<0.01 vs Dox group. Sample sizes (n): Con=10, Dox=7, ZXF=8, Cap=7.

ZXF Regulated the PI3K/PDK1/AKT/FoxO1 Signaling Pathway

To elucidate the mechanisms underlying ZXF's protective effects against HF, we performed phosphoprotein profiling using the CSP100plus signaling phospho-antibody microarray (Figure 9A). Compared with the control group, 16 phosphorylated proteins were upregulated, while 3 were downregulated in the Dox group. Following ZXF intervention, 10 phosphorylated proteins were upregulated, and 5 were downregulated (Supplementary Table S3). Comparative analysis revealed a 0.8-fold and 0.74-fold downregulation of PDK1 (Phospho-Ser241) and FOXO1/3/4-pan (Phospho-Thr24/32), respectively, in the Dox group relative to the control group. Following ZXF treatment, PDK1-Phospho levels increased by 1.75-fold, and FOXO1/3/4-pan-Phospho levels were upregulated by 1.34-fold (Figure 9B–D). These alterations are linked to key signaling pathways, including PI3K-Akt, Insulin, and AMPK. Building on the findings of the network pharmacology analysis, we further investigated the PI3K-Akt pathway to elucidate whether ZXF exerts its therapeutic effects through modulation of the PI3K/PDK1/AKT/FOXO1 signaling axis.

To validate this hypothesis, we conducted Western blot analysis to assess protein expression levels within the PI3K/PDK1/AKT/FOXO1 signaling pathway. As illustrated in Figure 10A–E, the expression levels of p-PI3K, p-PDK1, p-AKT, and p-FOXO1 were significantly downregulated in the model group compared to the control group. Notably, ZXF treatment markedly reversed these reductions, indicating that ZXF effectively restores the activity of the PI3K/PDK1/AKT/FOXO1 signaling axis.

Discussion

Heart failure is characterized by cardiomyocyte necrosis and myocardial fibrosis, manifesting as excessive collagen deposition, abnormal cardiac biomarkers, weakened myocardial contraction, and impaired diastolic filling.[2] These pathological changes progressively deteriorate cardiac function, ultimately leading to fatal outcomes.[20] Current HF treatment relies on pharmacological therapies, including beta-blockers, angiotensin-converting enzyme inhibitors (ACEIs), angiotensin II receptor blockers (ARBs), and mineralocorticoid receptor antagonists (MRAs). Newer agents

https://doi.org/10.2147/DDDT.S513643

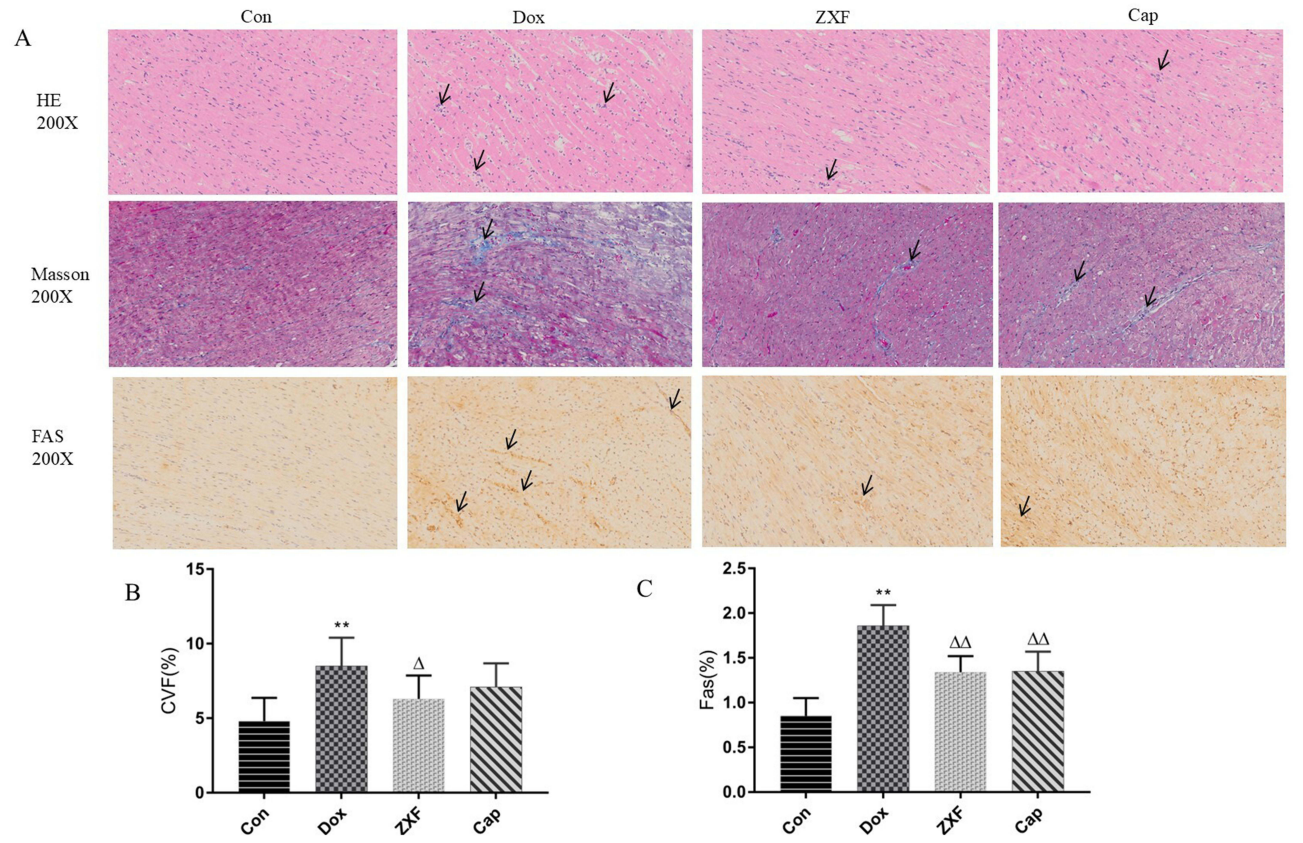

Figure 7 ZXF attenuated cardiac fibrosis and inflammation. (n=5). (**A**) Representative images of HE staining, Masson's staining and Immunohistochemical staining of FAS; (**B**) Statistical results of CVF (%). (**C**) Statistical results of Fas protein expression levels (%). $^{**}P<0.01$ vs Con group; $^{\Delta\Delta}P<0.01$ vs Dox group. Black arrows indicate characteristic histopathological changes, with their number reflecting lesion severity. Histochemistry analysis, magnification: 200×; scale=50 μm.

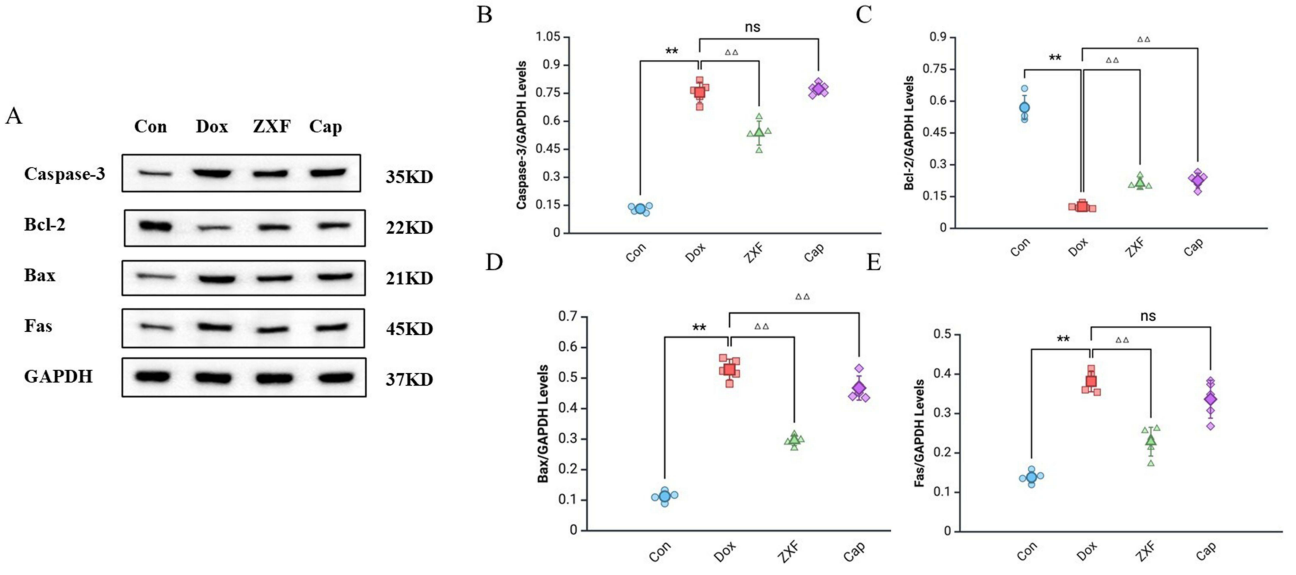

Figure 8 ZXF inhibited cardiomyocyte apoptosis. (n=5). (**A**) Western blot of protein levels of Caspase-3, Bcl-2, Bax and Fas. (**B**–**E**) Statistical results of Caspase-3/GAPDH, Bcl-2/GAPDH, Bax/GAPDH and Fas/GAPDH. $^{**}P<0.01$ vs Con group; $^{\Delta\Delta}P<0.01$, $^{ns}P>0.05$ vs Dox group.

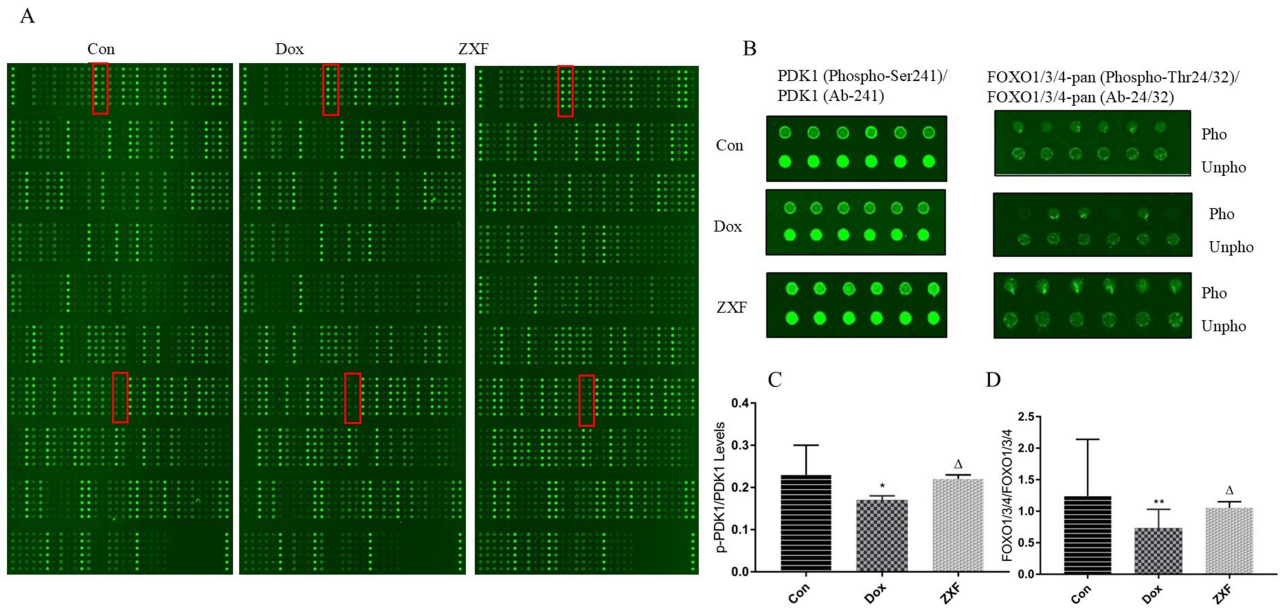

Figure 9 Phospho-Antibody array results showing the regulatory effects of ZXF on HF. (n=6). (**A**) The overview of phospho-antibody array results. (**B**) The figure of PDK1 (Phospho-Ser241), PDK1 (Ab-241), FOXO1/3/4-pan (Phospho-Thr24/32) and FOXO1/3/4-pan (Ab-24/32). (**C** and **D**) Statistical results of p-PDK1/PDK1, and p-FOXO1/3/4/FOXO1/3/4. **P*<0.05, ***P*<0.01 vs Con group; $^{\Delta}$*P*<0.05 vs Dox group.

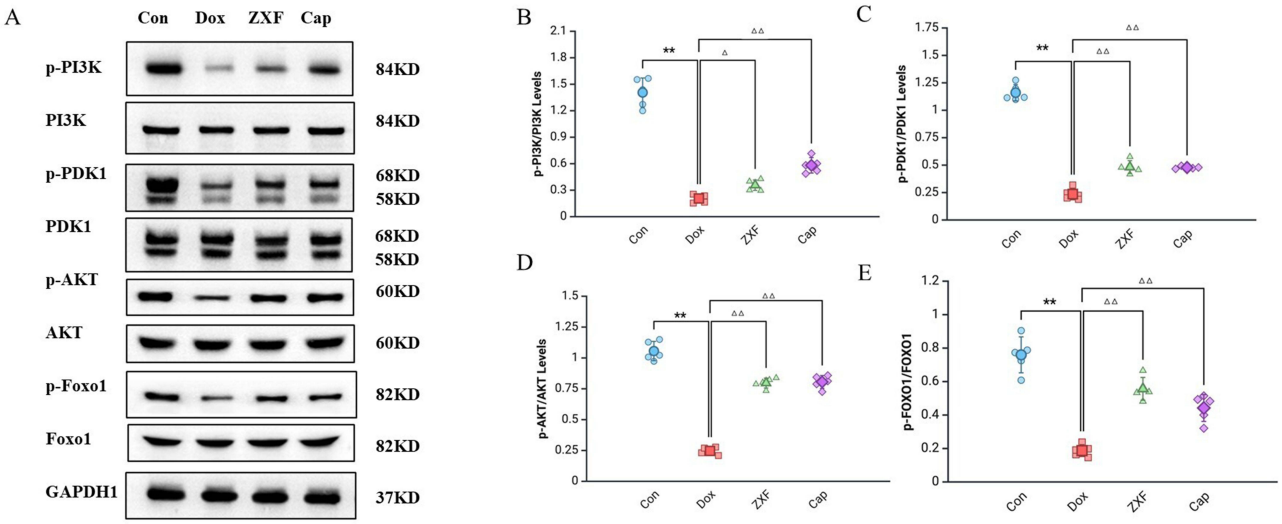

Figure 10 ZXF regulated the PI3K/PDK1/AKT/FoxO1 signaling pathway. (n=5). (**A**) Western blot of phosphorylated and total protein levels of PI3K, PDK1, AKT, and FOXO1. (**B**–**E**) Statistical results of p-PI3K/PI3K, p-PDK1/PDK1, p-AKT/AKT, and p-FOXO1/FOXO1. ***P*<0.01 vs Con group; $^{\Delta}$*P*<0.05, $^{\Delta\Delta}$*P*<0.01 vs Dox group.

such as angiotensin receptor-neprilysin inhibitors (ARNIs), sodium-glucose cotransporter-2 inhibitors (SGLT2i), and soluble guanylate cyclase stimulators (sGCs) have further improved patient outcomes.[4,21,22] However, these therapies are limited by side effects like hypotension and renal impairment and do not fully address underlying processes such as apoptosis, oxidative stress, and inflammation.[23–25]

Given these limitations, TCM offers a promising complementary approach by targeting these pathophysiological processes while enhancing cardiac function. TCM supports myocardial recovery and mitigates the side effects of conventional therapies, providing a more holistic strategy for HF management.[7,26,27] ZXF is a TCM formula employed by Longhua Hospital affiliated to Shanghai University of TCM for preventing and treating chronic HF. It is renowned for its ability to warm and nourish heart yang, transform qi, and promote diuresis. Numerous studies suggest that yang-

https://doi.org/10.2147/DDDT.S513643

warming prescriptions can alleviate hypotension,[28] and clinical research supports ZXF's potential anti-HF effects.[8] Furthermore, previous animal experiments have demonstrated that ZXF improves cardiac function and mitigates ventricular remodeling in heart failure models.[29] However, the precise molecular mechanisms underlying its therapeutic effects remain unclear.

Using network pharmacology, we identified 56 active compounds in ZXF and 752 genes linked to 1206 HF-related disease targets. Cross-referencing these disease and compound targets revealed 120 overlapping targets. GO and KEGG pathway enrichment analyses identified 159 associated signaling pathways, including AGE-RAGE, HIF-1, and Relaxin pathways, which are involved in oxidative stress, inflammation, energy metabolism, angiogenesis, apoptosis, and tissue remodeling—key processes underlying cardiovascular diseases, hypoxia-related disorders, and fibrosis.[30–32] PPI network analysis highlighted the top 20 ranked targets, with AKT1 emerging as the most significant, emphasizing its central role in regulating associated signaling pathways. PI3K, an essential upstream regulator of AKT, is a critical component of the PI3K-AKT signaling pathway, which governs fundamental biological processes such as apoptosis, cell survival, metabolism, and growth.[33,34] Our preliminary animal experiments with ZXF indicate its potential to improve ventricular remodeling, likely through the mitigation of cardiomyocyte apoptosis.[29] These findings direct our focus toward apoptosis-related mechanisms, particularly the PI3K-AKT signaling pathway, for further research.

DOX is a highly cardiotoxic drug that can lead to thinning of the ventricular wall, ventricular dilation, and a decrease in the ejection fraction, ultimately progressing to chronic heart failure.[35,36] Our study shows that DOX treatment results in severe cardiac dysfunction, myocardial hypertrophy, necrosis, fibrosis, and apoptosis in mice, while treatment with ZXF effectively improves these conditions. To further investigate ZXF's anti-apoptotic mechanisms, we employed the CSP100plus phospho-antibody array, which includes 304 phosphorylated proteins across 16 classical pathways. This high-throughput technology allows for the simultaneous detection and quantification of multiple phosphorylated proteins, offering a comprehensive overview of dynamic signaling changes.[13,37] Comparative analysis revealed downregulation of PDK1-Phospho and FOXO1/3/4-Phospho in the DOX group compared to controls, while ZXF treatment significantly restored their levels. Based on integrated findings from network pharmacology validation and CSP100plus phospho-antibody array analysis, we identified four crucial targets: PI3K, AKT, PDK1, and FOXO1. Previous studies have established their interconnected regulatory relationships: PI3K phosphorylates PIP2 to generate PIP3; PIP3 then recruits downstream signaling proteins including the serine/threonine kinase AKT; Activated AKT phosphorylates multiple substrates, including FOXO1.[38,39] Therefore, we propose that ZXF may exert its therapeutic effects on doxorubicin-induced heart failure through modulation of the PI3K/PDK1/AKT/FOXO1 pathway. This hypothesis was further validated by Western blot analysis, which showed that ZXF enhanced the phosphorylation levels of PI3K, PDK1, AKT, and FOXO1 in the DOX-induced heart failure model.

The PI3K/PDK1/AKT/FoxO1 signaling pathway is intricately linked to cardiomyocyte apoptosis (Figure 11). PDK1, also known as 3-phosphoinositide-dependent protein kinase 1, is a crucial signal transduction protein. As a key upstream activator of AKT, PDK1 regulates AKT activity and protects cardiomyocytes from apoptosis following HF.[40,41] In response to signaling cues, phosphatidylinositol-3,4,5-trisphosphate (PIP3) is generated by PI3K and accumulates on the inner surface of the cell membrane. PIP3 then binds to the N-terminal PH domain of AKT, inducing conformational changes that facilitate PDK1 binding and subsequent phosphorylation of AKT at the T308 activation site.[42] Once activated, AKT phosphorylates various substrates, including members of the FoxO (Forkhead box O) family, such as FoxO1, FoxO3, and FoxO4 (collectively referred to as FoxO1/3/4).[43–45] Among them, FoxO1 is the most extensively studied. Moderate activation of FoxO1 helps resist oxidative stress and maintain cellular homeostasis, while excessive activation can induce apoptosis and myocardial fibrosis.[46,47] Phosphorylation of FoxO1 by AKT causes its translocation from the nucleus to the cytoplasm, thereby reducing its ability to activate pro-apoptotic genes such as Bim, FasL, and Caspase-3. This translocation also enhances AKT-mediated survival signals by inhibiting pro-apoptotic proteins like Bax, suppressing mitochondrial apoptotic pathways, and decreasing cytochrome C release and Caspase-3 activation.[48,49] Furthermore, cytoplasmic FoxO1 helps maintain oxidative stress balance, thereby reducing apoptosis caused by oxidative damage.[50,51] Together, these mechanisms protect cardiomyocytes, reduce apoptosis, alleviate myocardial damage, improve cardiac function, and slow the progression of heart failure.[52,53]

Collectively, these findings suggest that ZXF mitigates DOX-induced HF by modulating the PI3K/PDK1/AKT/FOXO1 signaling pathway. Given the central role of this pathway in cardiomyocyte survival, its regulation by ZXF provides not only mechanistic insight but also a promising foundation for clinical translation. These data support the

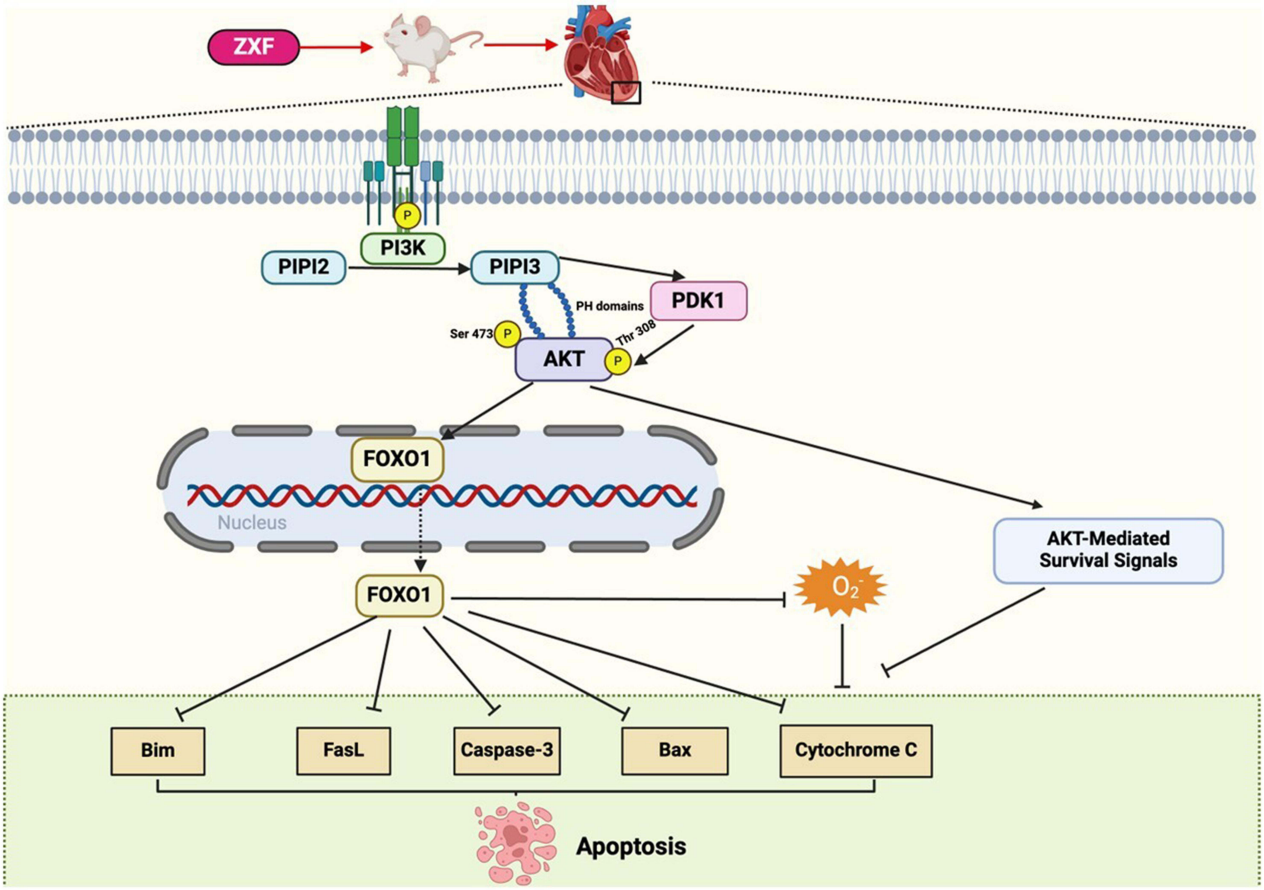

Figure 11 Illustration of the PI3K/PDK1/AKT/FoxO1 Signaling Pathway in Inhibiting Cardiomyocyte Apoptosis and the Role of ZXF.

potential utility of ZXF or its active components as adjunctive therapies to counteract Dox-related cardiotoxicity in cancer patients or to improve outcomes in heart failure. However, several limitations should be acknowledged. Firstly, the relatively small sample size in each group may limit the robustness of our conclusions, and thus future studies with larger cohorts are warranted. Secondly, while network pharmacology provides useful insights, it relies heavily on existing databases and preclinical models, which may not fully capture the complexity and dynamic nature of human pathophysiology. Lastly, the doxorubicin-induced heart failure model used here represents one of many etiologies of heart failure. Since heart failure can arise from diverse causes including ischemic injury, hypertension, valvular heart disease, and genetic cardiomyopathies, the findings may not be universally applicable across all types of heart failure.

Conclusion

In summary, our study investigates the role and mechanisms of ZXF in alleviating DOX-induced HF by combining network pharmacology, phospho-antibody array analysis, and experimental validation. Our findings reveal that ZXF effectively mitigates ventricular remodeling, reduces cardiomyocyte apoptosis, and alleviates myocardial fibrosis in DOX-induced HF rats, mediated through the regulation of the PI3K/PDK1/AKT/FoxO1 signaling pathway.

Ethical Approval

The animal study was approved by the Experimental Animal Ethics Committee of Shanghai University of TCM and adhered to the IACUC guidelines (Permit Number: PZSHUTCM210312009).

Author Contributions

All authors made a significant contribution to the work reported, whether that is in the conception, study design, execution, acquisition of data, analysis and interpretation, or in all these areas; took part in drafting, revising or critically reviewing the article; gave final approval of the version to be published; have agreed on the journal to which the article has been submitted; and agree to be accountable for all aspects of the work.

Funding

This research was supported by the National Natural Science Foundation of China (No.82374397, NO.82004319), Shanghai Municipal Health Commission Talent Program (2022YQ040), and the fifth batch of the Talent Program (The Education Correspondence of National Chinese Medicine Industry [2022] No. 1).

Disclosure

The authors confirmed that there are no conflicts of interest related to this publication.

References

1. Baman JR, Ahmad FS. Heart failure. *JAMA*. 2020;324(10):1015. doi:10.1001/jama.2020.13310
2. McDonagh TA, Metra M, Adamo M, et al. 2021 ESC Guidelines for the diagnosis and treatment of acute and chronic heart failure. *Eur Heart J*. 2021;42(36):3599–3726. doi:10.1093/eurheartj/ehab368
3. Chang AJ, Liang Y, Girouard MP, et al. Changing the paradigm in heart failure: shifting from treatment to prevention. *Heart Fail Rev*. 2024;30(1):177–189. doi:10.1007/s10741-024-10454-2
4. Heidenreich PA, Bozkurt B, Aguilar D, et al. 2022 AHA/ACC/HFSA guideline for the management of heart failure: a Report of the American College of Cardiology/American Heart Association Joint Committee on Clinical Practice Guidelines. *Circulation*. 2022;145(18):e895–e1032. doi:10.1161/cir.0000000000001063
5. Suo YF, IokFai XH, Zhang HF, Li XL. [Effectiveness and safety of traditional Chinese medicine for heart failure management]. *Zhonghua Xin Xue Guan Bing Za Zhi*. 2024;52(9):980–984. Polish. doi:10.3760/cma.j.cn112148-20231019-00346
6. Guo L, Yang Z, Feng W, et al. Clinical evidence and potential mechanisms of traditional Chinese medicine for refractory heart failure: a literature review and perspectives. *Front Cardiovasc Med*. 2024;11:1369642. doi:10.3389/fcvm.2024.1369642
7. Cheang I, Yao W, Zhou Y. The traditional Chinese medicine Qiliqiangxin in heart failure with reduced ejection fraction: a randomized, double-blind, placebo-controlled trial. *Nat Med*. 2024;30(8):2295–2302. doi:10.1038/s41591-024-03169-2
8. Cao M, Wang YH, Yang AL, et al. Clinical observation of Zhenxin Fang in the treatment of chronic heart failure. *J Integr Tradit Chin West Med Cardiovasc Cerebrovasc Dis*. 2019;17(23):3662–3665. doi:10.12102/j.issn.1672-1349.2019.23.004
9. Duan X, Wang N, Peng D. Application of network pharmacology in synergistic action of Chinese herbal compounds. *Theory Biosci*. 2024;143(3):195–203. doi:10.1007/s12064-024-00419-2
10. Liu Y, Li X, Chen C, Ding N, Ma S, Yang M. Exploration of compatibility rules and discovery of active ingredients in TCM formulas by network pharmacology. *Chin Herb Med*. 2024;16(4):572–588. doi:10.1016/j.chmed.2023.09.008
11. Jiashuo WU, Fangqing Z, Zhuangzhuang LI, Weiyi J, Yue S. Integration strategy of network pharmacology in Traditional Chinese Medicine: a narrative review. *J Tradit Chin Med*. 2022;42(3):479–486. doi:10.19852/j.cnki.jtcm.20220408.003
12. Terfve C, Saez-Rodriguez J. Modeling signaling networks using high-throughput phospho-proteomics. *Advances in Experimental Medicine and Biology*. 2012;736:19–57. doi:10.1007/978-1-4419-7210-1_2
13. Heimburg-Molinaro J, Mehta AY, Tilton CA, Cummings RD. Insights into glycobiology and the protein-glycan interactome using glycan microarray technologies. *Mol Cell Proteomics*. 2024;23(11):100844. doi:10.1016/j.mcpro.2024.100844
14. He ML, Li XY, Guo YQ, et al. Nerol attenuates doxorubicin-induced heart failure by inhibiting cardiomyocyte apoptosis in rats. *Eur J Pharmacol*. 2025;987:177203. doi:10.1016/j.ejphar.2024.177203
15. Wu Q, Dong Y, Ma M, et al. Effect of Kuoxin recipe on myocardial apoptosis in doxorubicin-induced dilated cardiomyopathy rats via regulating ASK1/JNK/Cx43 signaling pathway. *Lishizhen Med Mater Med Res*. 2024;35(15):3340–3347. doi:10.3969/j.issn.1008-0805.2024.15.06
16. Dong Y, Ma M, Peng L, et al. Impaired cardiac lymphangiogenesis in doxorubicin-induced dilated cardiomyopathy mice and the therapeutic effect of Kuoxin recipe. *World Sci Technol-Modern Tradit Chin Med*. 2023;25(10):3293–3303. doi:10.11842/wst.20230905001
17. Meng XM, Pang QY, Zhou ZF, et al. Histone methyltransferase MLL4 protects against pressure overload-induced heart failure via a THBS4-mediated protection in ER stress. *Pharmacol Res*. 2024;205:107263. doi:10.1016/j.phrs.2024.107263
18. Jarabicová I, Horváth C, Hrdlička J, et al. Necrosis-like cell death modes in heart failure: the influence of aetiology and the effects of RIP3 inhibition. *Basic Res Cardiol*. 2025;120(2):373–392. doi:10.1007/s00395-025-01101-4
19. Weng H, Zou W, Tian F, et al. Inhalable cardiac targeting peptide modified nanomedicine prevents pressure overload heart failure in male mice. *Nat Commun*. 2024;15(1):6058. doi:10.1038/s41467-024-50312-1
20. Park AC, Mann DL. The pathobiology of myocardial recovery and remission: from animal models to clinical observations in heart failure patients. *Methodist DeBakey Cardiovasc J*. 2024;20(4):16–30. doi:10.14797/mdcvj.1389
21. Haghighat L, DeJong C, Teerlink JR. New and future heart failure drugs. *Nat Cardiovasc Res*. 2024;3(12):1389–1407. doi:10.1038/s44161-024-00576-z
22. Colombo G, Biering-Sorensen T, Ferreira JP, et al. Cardiac remodelling in the era of the recommended four pillars heart failure medical therapy. *ESC Heart Fail*. 2024;12(2):1029–1044. doi:10.1002/ehf2.15095

23. Al-Mohammad A. ARNI-induced hypotension in HFrEF: a feared side-effect or a marker of modifiable risk? *J Am Coll Cardiol*. 2024;84 (18):1701–1703. doi:10.1016/j.jacc.2024.08.054
24. Wang Y, Liu X. A real-world disproportionality analysis of sacubitril/valsartan: data mining of the FDA adverse event reporting system. *Front Pharmacol*. 2024;15:1392263. doi:10.3389/fphar.2024.1392263
25. Stompór T, Winiarska A. Kidneys in heart failure: impact of flozins. *Kardiol Pol*. 2023;81(11):1071–1080. doi:10.33963/v.kp.97844
26. Wei H, Wu H, Yu W, Yan X, Zhang X. Shenfu decoction as adjuvant therapy for improving quality of life and hepatic dysfunction in patients with symptomatic chronic heart failure. *J Ethnopharmacol*. 2015;169:347–355. doi:10.1016/j.jep.2015.04.016
27. Pan G, Ji W, Wang X. Effects of multifaceted optimization management for chronic heart failure: a multicentre, randomized controlled study. *ESC Heart Fail*. 2023;10(1):133–147. doi:10.1002/ehf2.14170
28. Guo L, Yuan H, Zhang D, et al. A multi-center, randomized, double-blind, placebo-parallel controlled trial for the efficacy and safety of shenfuqiangxin pills in the treatment of chronic heart failure (Heart-Kidney yang deficiency syndrome). *Medicine*. 2020;99(21):e20271. doi:10.1097/md.0000000000020271
29. Li SC, Zhou L, Zhu LY, et al. The effects of Zhenxin Fang on cardiac function, ventricular remodeling, and energy metabolism in pressure overload-induced heart failure rats. *World Clin Drugs*. 2024;45(06):597–602. doi:10.13683/j.wph.2024.06.005
30. Wang B, Jiang T, Qi Y, et al. AGE-RAGE axis and cardiovascular diseases: pathophysiologic mechanisms and prospects for clinical applications. *Cardiovasc Drugs Ther*. 2024:1–8. doi:10.1007/s10557-024-07639-0
31. Mialet-Perez J, Belaidi E. Interplay between hypoxia inducible Factor-1 and mitochondria in cardiac diseases. *Free Radic Biol Med*. 2024;221:13–22. doi:10.1016/j.freeradbiomed.2024.04.239
32. Sassoli C, Nistri S, Chellini F, Bani D. Human recombinant relaxin (Serelaxin) as anti-fibrotic agent: pharmacology, limitations and actual perspectives. *Curr Mol Med*. 2022;22(3):196–208. doi:10.2174/1566524021666210309113650
33. Ghafouri-Fard S, Khanbabapour Sasi A, Hussen BM. Interplay between PI3K/AKT pathway and heart disorders. *Mol Biol Rep*. 2022;49 (10):9767–9781. doi:10.1007/s11033-022-07468-0
34. Qin W, Cao L, Massey IY. Role of PI3K/Akt signaling pathway in cardiac fibrosis. *Mol Cell Biochem*. 2021;476(11):4045–4059. doi:10.1007/s11010-021-04219-w
35. Li Y, Yan J, Yang P. The mechanism and therapeutic strategies in doxorubicin-induced cardiotoxicity: role of programmed cell death. *Cell Stress Chaperones*. 2024;29(5):666–680. doi:10.1016/j.cstres.2024.09.001
36. Avagimyan A, Pogosova N, Kakturskiy L. Doxorubicin-related cardiotoxicity: review of fundamental pathways of cardiovascular system injury. *Cardiovasc Pathol*. 2024;73:107683. doi:10.1016/j.carpath.2024.107683
37. Ling S, Xie H, Yang F. Metformin potentiates the effect of arsenic trioxide suppressing intrahepatic cholangiocarcinoma: roles of p38 MAPK, ERK3, and mTORC1. *J Hematol Oncol*. 2017;10(1):59. doi:10.1186/s13045-017-0424-0
38. He Y, Sun MM, Zhang GG. Targeting PI3K/Akt signal transduction for cancer therapy. *Signal Transduct Target Ther*. 2021;6(1):425. doi:10.1038/s41392-021-00828-5
39. Burke JE, Triscott J, Emerling BM, Hammond GRV. Beyond PI3Ks: targeting phosphoinositide kinases in disease. *Nat Rev Drug Discov*. 2023;22 (5):357–386. doi:10.1038/s41573-022-00582-5
40. He L, Feng H, Yin B, et al. Sodium new houttuyfonate induces apoptosis of breast cancer cells via ROS/PDK1/AKT/GSK3β axis. *Cancers*. 2023;15(5):1614. doi:10.3390/cancers15051614
41. Yuan L, Ji H-G, Yan X-J, Liu M, Ding Y-H, Chen X-H. Dioscin ameliorates doxorubicin-induced heart failure via inhibiting autophagy and apoptosis by controlling the PDK1-mediated Akt/mTOR signaling pathway. *Kaohsiung J Med Sci*. 2023;39(10):1022–1029. doi:10.1002/kjm2.12740
42. Hu S-H, He X-D, Nie J. Methylene-bridge tryptophan fatty acylation regulates PI3K-AKT signaling and glucose uptake. *Cell Rep*. 2022;38 (11):110509. doi:10.1016/j.celrep.2022.110509
43. Tzivion G, Dobson M, Ramakrishnan G. FoxO transcription factors; regulation by AKT and 14-3-3 proteins. *Biochim Biophys Acta*. 2011;1813 (11):1938–1945. doi:10.1016/j.bbamcr.2011.06.002
44. Sengupta A, Molkentin JD, Paik JH, DePinho RA, Yutzey KE. FoxO transcription factors promote cardiomyocyte survival upon induction of oxidative stress. *J Biol Chem*. 2011;286(9):7468–7478. doi:10.1074/jbc.M110.179242
45. Li H, Yang W, Shang Z, et al. Dehydrocorydaline attenuates myocardial ischemia-reperfusion injury via the FoXO signalling pathway: a multimodal study based on network pharmacology, molecular docking, and experimental study. *J Ethnopharmacol*. 2025;337(Pt 1):118738. doi:10.1016/j.jep.2024.118738
46. Zhang X, Jiang L, Liu H. Forkhead box protein O1: functional diversity and post-translational modification, a new therapeutic target? *Drug Des Devel Ther*. 2021;15:1851–1860. doi:10.2147/dddt.S305016
47. Sun Z, Li P, Wang X, et al. GLP-1/GLP-1R signaling regulates ovarian PCOS-associated granulosa cells proliferation and antiapoptosis by modification of forkhead box protein O1 phosphorylation sites. *Int J Endocrinol*. 2020;2020:1484321. doi:10.1155/2020/1484321
48. Lei Z, Ali I, Yang M, Yang C, Li Y, Li L. Non-esterified fatty acid-induced apoptosis in bovine granulosa cells via ROS-activated PI3K/AKT/FoxO1 pathway. *Antioxidants*. 2023;12(2):434. doi:10.3390/antiox12020434
49. Jafari-Azad A, Hosseini L, Rajabi M, et al. Nicotinamide mononucleotide and melatonin counteract myocardial ischemia-reperfusion injury by activating SIRT3/FOXO1 and reducing apoptosis in aged male rats. *Mol Biol Rep*. 2021;48(4):3089–3096. doi:10.1007/s11033-021-06351-8
50. Wang K, Zhang W, Liu J, Cui Y, Cui J. Piceatannol protects against cerebral ischemia/reperfusion-induced apoptosis and oxidative stress via the Sirt1/FoxO1 signaling pathway. *Mol Med Rep*. 2020;22(6):5399–5411. doi:10.3892/mmr.2020.11618
51. Ning Y, Li Z, Qiu Z. FOXO1 silence aggravates oxidative stress-promoted apoptosis in cardiomyocytes by reducing autophagy. *J Toxicol Sci*. 2015;40(5):637–645. doi:10.2131/jts.40.637
52. Sun Y, Liu Y, Cai Y, Han P, Hu S, Cao L. Atractylenolide I inhibited the development of malignant colorectal cancer cells and enhanced oxaliplatin sensitivity through the PDK1-FoxO1 axis. *J Gastrointest Oncol*. 2022;13(5):2382–2392. doi:10.21037/jgo-22-910
53. Lee JH, Jeon J, Bai F, Wu W, Ha UH. Negative regulation of interleukin 1β expression in response to DnaK from Pseudomonas aeruginosa via the PI3K/PDK1/FoxO1 pathways. *Comp Immunol Microbiol Infect Dis*. 2020;73:101543. doi:10.1016/j.cimid.2020.101543